Research Paper

Metabolic adaptation and oxaloacetate homeostasis in *P. fluorescens* exposed to aluminum toxicity

Joseph Lemire, Puja Kumar, Ryan Mailloux, Kathyrn Cossar and Vasu D. Appanna

Department of Chemistry and Biochemistry, Laurentian University, Sudbury, Ontario, Canada

Microbial systems are known to elaborate intricate metabolic strategies in an effort to fend the toxic impact of numerous metals. In this study, we show that the exposure of *Pseudomonas fluorescens* to aluminum (Al) resulted in a metabolic shift aimed at diverting oxaloacetate towards the biogenesis of an aluminophore. This metabolic alteration was characterized by uncoupling of two gluconeogenic enzymes, namely pyruvate carboxylase (PC) and phosphoenolpyruvate carboxykinase (PEPCK). While PC displayed a sharp increase in activity and expression, PEPCK was severely diminished. Malic enzyme (ME) and NAD kinase (NADK), two enzymes involved in maintaining a reductive environment, were markedly increased in the Al-stressed cells. Hence, Al-exposed *Pseudomonas fluorescens* evoked a metabolic response aimed at generating oxaloacetate and promoting an intracellular reductive environment.

Keywords: Aluminum toxicity / Oxaloacetate / Pyruvate carboxylase / Metabolic shift

Received: January 07, 2008; accepted: February 02, 2008

DOI 10.1002/jobm.200800007

Introduction

Despite its ubiquity, Al contributes to no known role in biological processes. Indeed, this trivalent metal has been excluded from biological systems due the unfavourable aspects of its chemistry. Although Al insolubility at neutral pH prevents its biological uptake, industrial activities, pollution, and acid rain have increased the bioavailability of this trivalent metal. Al is reputed for its toxic influence on various biological systems. Membrane bilayers, Ca-mediated reactions, and Mg binding sites are known targets for the toxicity of Al [1]. Furthermore, Al also competes for Fe binding sites in several enzyme active sites and promotes oxidative stress [2]. Neurological disorders, obesity, and stunted root growth have been attributed to the toxic effects of Al [3]. Thus, the presence of Al within an organism can be catastrophic since it can perturb macromolecular structures, disrupt Fe homeostasis, and promote oxidative stress [4].

Due to the adverse attributes of Al, many organisms have adopted a battery of protective mechanisms in order to mitigate the toxicity of this metal pollutant [5]. Various metabolic pathways have been shown to converge and act in a synergistic fashion in order to nullify Al and quell its pro-oxidant properties. For instance, tobacco plants are well known to invoke a metabolic shift aimed at the production of citrate, a potent chelator of Al [6]. Following its complexation, the Al-citrate complex is effluxed from the organism. In fact, the ability of tobacco to resist the toxic affects of Al has prompted the generation of Al-resistant crops [7]. Bacteria, such as *Pseudomonas fluorescens*, also alter several metabolic networks in order to cope with Al toxicity. For instance, exposure to Al provokes a metabolic shift in this gram-negative soil microbe aimed at producing oxalate, a dicarboxylic acid known to sequester Al. Enhanced expression of isocitrate lyase (ICL) enables the organism to generate glyoxylate that is subsequently converted into oxalate [8]. Phosphatidyl ethanolamine (PE) also appears to play a pivotal role in this detoxification strategy [9]. However, if the phosphate level is decreased 100-fold, *P. fluorescens* produces a polycarboxylate-citrate derivative as an aluminophore, an aluminum sequestering molecule [10, 11]. In this instance, the condensation of acetyl CoA mediated by citrate synthase (CS) is instrumental in the biogenesis of the aluminophore [11]. However, the generation of

Correspondence: Vasu D. Appanna, Department of Chemistry and Biochemistry, Laurentian University, Sudbury, Ontario P3E 2C6, Canada
E-mail: VAppanna@laurentian.ca
Phone: 705-675-1151 (Ext. 2112)
Fax: 705-675-4844

oxaloacetate, the other ingredient necessary for this process is not fully understood.

In this report, we demonstrate that the increased expression of PC and the decreased expression of PEPCK contributed to oxaloacetate homeostasis in Al-stressed cells. Although these enzymes work together in the gluconeogenic pathway, this microbe uncoupled the activity of these two enzymes in order to maintain a pool of oxaloacetate for the production of the aluminophore. The metabolic response elicited in response to Al toxicity also included the participation of ME and NADK. The roles of these enzymes and the metabolic networks that allowed *Pseudomonas fluorescens* to combat Al stress are also discussed.

Materials and methods

Microbial growth conditions

Pseudomonas fluorescens (ATCC 13525) was obtained from the American Type Culture Collection and was maintained and grown in a mineral medium consisting of Na_2HPO_4 (0.06 g), KH_2PO_4 (0.03 g), NH_4Cl (0.8 g), $MgSO_4 \cdot 7\ H_2O$ (0.2 g), and 20 mM citrate (2.7 g) per litre of deionized water. Trace elements were present in concentrations as described previously [12]. In the Al-stressed medium, citrate was complexed to 15 mM $AlCl_3 \cdot 6H_2O$. The pH was adjusted to 6.8 with 1N NaOH. The media was then dispensed into 200 ml amounts in 500 ml Erlenmeyer flasks, stoppered with foam plugs, and autoclaved for 20 min at 121 °C. The media were inoculated with 1ml of stationary-phase cells grown in an Al-free medium in an aerated gyratory water bath shaker, model 76 (New Brunswick Scientific) at 26 °C at 140 rpm. Cells were isolated at similar growth phases (control: 24 h, Al-stressed: 30 h) for enzymatic and HPLC analyses.

Cellular fractionation

The bacterial cells were harvested at similar growth phases (24 h for control and 30 h for Al-stressed) and then resuspended in a cell storage buffer (CSB) consisting of 50 mM Tris-HCl, 5 mM $MgCl_2$, 1 mM PMSF (pH 7.3). The cells were disrupted by sonication and then centrifuged at 3,000 × *g* for 30 min at 4 °C to remove intact bacteria. Centrifugation at 180,000 × *g* for 2 h afforded a soluble cell free extract (CFE) and a membrane CFE. The soluble fraction was further centrifuged at 180,000 × *g* for 1 h to afford a membrane-free system. The protein content in the soluble and membrane fractions was determined using the Bradford assay [13]. These CFE fractions were kept at 4 °C for up to 5 days and various enzymatic activities were monitored.

Enzymatic assays

Specific activity of PEPCK was determined using the 2,4-dinitrophenyl hydrazine (DNPH) assay as described in [14]. A 0.2 mg equivalent to soluble CFE was incubated for 300 sec in a reaction buffer (25 mM Tris-HCl (pH 7.3), 5 mM $MgCl_2$) containing 2 mM PEP, 0.25 mM GDP, and 2 mM HCO_3^-. The production of oxaloacetate was monitored at 450 nm.

Blue Native (BN) PAGE and in-gel activity staining

Blue Native (BN) PAGE was performed according to a modified method as described previously [15, 16]. Cellular fractions isolated from *P. fluorescens* were prepared in a native buffer (50 mM Bis-Tris, 500 mM ε-aminocaproic acid, pH 7.0, 4 °C) at a final concentration of 4 mg of protein per ml. For the membrane CFE, 1% (v/v) β-dodecyl-D-maltoside was included in the preparation in order to solubilize the membrane-bound protein. To ensure optimal protein separation, 4–16% linear gradient gels were cast with the Bio-Rad MiniProtean™ 2 system using 1 mm spacers. 60 μg of soluble or membrane protein was loaded into the wells and the gels were electrophoresed under native conditions. 80 V was applied for the stacking gel. The voltage was then increased to 300 V once the running front entered the separating gel. The blue cathode buffer (50 mM Tricine, 15 min Bis-Tris, 0.02% (w/v) Coomassie G-250 (pH 7) at 4 °C) was changed to a colorless cathode buffer (50 mM Tricine, 15 min Bis-Tris, (pH 7) at 4 °C) when the running front was half-way through the gel. Upon completion, the gel slab was equilibrated for 15 min in a reaction buffer. The in-gel visualization of enzyme activity was ascertained by coupling the formation of NAD(P)H to 0.3 mg/ml of phenazine methosulfate (PMS) and 0.5 mg/ml of iodonitrotetrazolium (INT). ME activity was visualized using a reaction mixture consisting of reaction buffer, 5 mM malate, 0.5 mM NADP, INT, and PMS. MDH was detected in a similar fashion except NADP was replaced with NAD. NADP-ICDH was also monitored with reaction buffer, 5 mM isocitate, 0.5 mM NADP, INT and PMS.

PEPCK activity was monitored with the aid of MDH. A reaction mixture consisting of 10 mM PEP, 1 mM ADP, 10 mM HCO_3^-, 5 units/ml MDH, 0.5 mM NADH, INT, 0.0167 mg/ml of 2,4-dichloroindophenol (DCIP) was employed to visualize the activity of this enzyme. We have previously employed DCIP in order to assess the in-gel activity of NADH oxidizing enzymes [16, 17]. PC was also monitored using a reaction mixture containing 5 mM pyruvate, 1 mM ATP, 5 mM HCO_3^-, 0.5 mM NADH, 8 units/ml MDH, DCIP, and INT. The activity of NAD kinase was ascertained using an en-

zyme coupled assay as described in [18]. NADK was made apparent using a reaction mixture containing 0.5 mM NAD, 3 mM ATP, 5 mM isocitrate, 1 unit/ml of NADP-ICDH, INT, and PMS. NDPK activity was assessed using a reaction mixture containing 0.75 mM ADP, 0.75 mM NADP, 15 mM glucose, 5 units HK, 5 units G6PDH, 1 mM GTP, INT, and PMS. Reactions were stopped using destaining solution (40% methanol, 10% glacial acetic acid) once the activity bands reached their desired intensities. The resulting bands were documented and used for 2D SDS-PAGE analysis. Activity stains performed in the absence of substrate assured band specificity. Proper protein loading was determined by coomassie staining for total proteins. The activities of ME, PEPCK, NADP-ICDH, NDPK, and NADK were monitored in soluble CFE while MDH and PC were analyzed in the membrane CFE. As the 24 h control cells and 30 h Al-stressed cells correspond to the same growth phase [10], they were selected for comparative enzymatic studies.

Two dimensional SDS-PAGE and silver staining

2D SDS-PAGE gels were performed in accordance with the modified method described in [19, 20]. For 2D SDS-PAGE analysis, activity bands from native gels were precision cut from the gel and incubated in denaturing buffer (1% β-mercaptoethanol, 5% SDS) for 30 min, and then loaded vertically into the SDS gel. 10% SDS gels were favoured for the separation of the proteins. Proteins were detected using silver staining kits purchased from Bio-Rad.

Regulation experiments

The Al-mediated regulation of PC and PEPCK was studied in the following manner. A 10 mg protein equivalent of Al-treated cells was transferred into a citrate (control) medium and a 10 mg protein equivalent of control cells was incubated in an Al-citrate (Al-stressed) containing medium. Following a 4 h incubation, the cells were isolated and fractionated as described previously for activity analysis. For proper comparison, control cells (24 h) and Al-stressed (30 h) were utilized to inoculate the different media, respectively.

Analysis of PEP and oxaloacetate levels

PEP and oxaloacetate levels were determined using HPLC. Cells from control and Al-stressed conditions isolated at similar growth phases were homogenized by sonication as described above and then subjected to HPLC analysis. A 2 mg equivalent to CFE was treated with 0.5% v/v perchloric acid for 10 min on ice and then the precipitate was removed by centrifugation. The supernatant was then filtered and injected into an Alliance HPLC equipped with a C_{18} reverse-phase column (Synergi Hydro-RP; 4 μm; 250 × 4.6 mm, Phenomenex) operating at a flow rate of 0.7 ml/min at ambient temperature. This flow rate was utilized for the identification of oxaloacetate. For the proper identification of PEP, a flow rate of 0.4 ml/min was applied to the HPLC. A mobile phase consisting of 20 mM K_2HPO_4 (pH 2.9) was used for the identification PEP and oxaloacetate. These organic acids were monitored at 210 nm. PEP and oxaloacetate were identified by injecting known standards individually and by spiking the various samples.

Statistical analysis

Data were expressed as means ± standard deviations. Statistical correlations of data were checked for significance using the Student *t*-test ($p \leq 0.05$). All experiments were performed twice and in triplicate.

Results and discussion

We have previously observed that Al-exposed *P. fluorescens* grown in a normal phosphate medium containing citrate produced a polycarboxylate-citrate derivative in order to detoxify this toxic metal. To probe the nature of this adaptation, we analyzed the metabolite content of the Al-stressed cells by HPLC. Cells exposed to Al contained two-fold less PEP in comparison to control cells (Table 1). In contrast, the Al-stressed cells yielded a numerous fold increase in oxaloacetate in comparison to control cells (Table 1). We have previously observed that the production of this aluminophore is dependent on the increased activity of CS, a key tricarboxylic acid (TCA) cycle enzyme which condenses oxaloacetate and acetyl CoA producing citrate [11]. In order to account for the diminished amount of PEP in the Al-exposed cells we tested the activity of PEPCK over a period of 35 h. Indeed, a sharp decrease in the specific activity of PEPCK was observed in the Al-treated cells incubated in Al for 35 h (Fig. 1, 1). In order to confirm the decrease PEPCK activity, we performed BN PAGE. Indeed, the intensity of the activity band in the Al-treated cells was diminished in contrast to the control cells (Fig. 1, 2). The diminished activity of PEPCK in the Al-treated cells was due to a dearth of available protein. Indeed, 2D SDS-PAGE analysis of the activity bands revealed a sharp decrease in the amount of PEPCK (Fig. 1, 3). To further evaluate the notion that Al reduced the activity of PEPCK, we exposed control cells to Al for 4 h. Control cells exposed to Al displayed a sharp decrease in PEPCK

Table 1. Relative metabolite levels in control and Al-stressed cells. Cells were isolated at similar growth phases and subjected to HPLC analysis.

Conditions	PEP	Oxaloacetate
Control	45724 ± 5287.8	4332 ± 345.8
Stress	27429 ± 1362.6*	37847 ± 4171.93*

Units are displayed as arbitrary absorbance units (AU) quantified by Empower software.

* Denotes a significant change between control and stressed cells Significance determined by student *T*-test, performed with 2 degrees of freedom at a 95% confidence interval

activity (Fig. 1, 4). In contrast, the PEPCK activity recovered in the Al-treated cells incubated in a control medium. This indicates that Al modulates the activity of this gluconeogenic enzyme. The activity of PEPCK is dependent on a steady supply of GTP or ATP. Thus, the in-gel activity of NDPK, an enzyme known to maintain the levels of nucleoside triphosphates, was monitored [21]. In contrast to control cultures, the Al-stressed cells displayed no apparent NDPK activity (Fig. 1, 5). Thus, the reduced activities of PEPCK and NDPK would indicate that oxaloacetate was not being converted to PEP effectively.

Since oxaloacetate appeared to be an important metabolite in the Al-exposed cells, the activity and expression of PC, a key enzyme involved in the homeostasis of this α-keto acid, was monitored. PC catalyzes the production of oxaloacetate by carboxylating pyruvate. In-gel activity analysis revealed that the activity of PC was increased in cells treated with Al (Fig. 2, 1). The increase in activity was associated with an enhanced amount of protein. Indeed, 2D SDS-PAGE analysis and silver staining revealed a higher amount of protein associated with the activity bands from the Al-treated cells (Fig. 2, 2). In order to probe the influence of this toxic trivalent metal on PC activity further, we exposed control cells to an Al-containing medium for 4 h. An increase in PC activity was observed following the incubation of control cells to Al (Fig. 2, 3). In contrast, Al-exposed cells cultured in control conditions for 4 h displayed a slight decrease in PC activity. However, after 12–24 h of incubation, the decrease became more pronounced (data not shown). Thus, PC is required to maintain the level of oxaloacetate for aluminophore production. PEPCK and PC usually participate in gluconeogenesis to produce intermediates for biosynthetic reactions. However, it appears that Al toxicity uncouples these two enzymes in order to generate in-

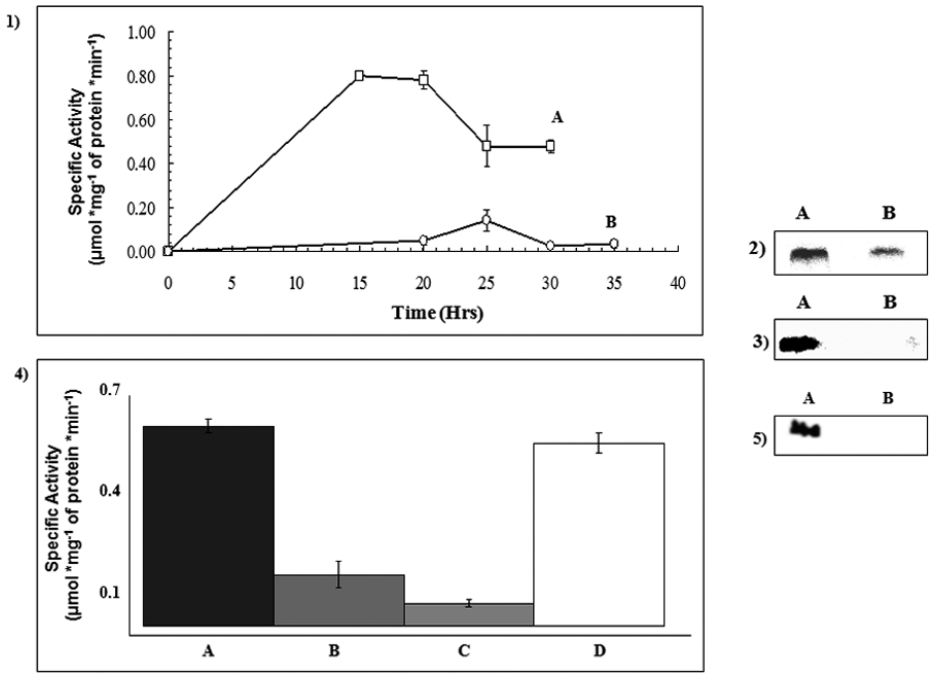

Figure 1. Activity and expression of PEPCK in cells exposed to A) control or B) Al-stressed conditions. 1) The specific activity of PEPCK at various growth intervals. 2) In-gel activity stain for PEPCK. 3) 2D SDS PAGE analysis of PEPCK expression. The activity bands from panel 2 were excised, treated with 1% SDS, and then electrophoresed under denaturing conditions. Protein was detected using the silver staining protocol. 4) The Al-mediated modulation of PEPCK activity: the specific activity of PEPCK for cells exposed to A) control, B) Al-stressed, C) control exposed to Al-stressed for 4 h, and D) Al-stressed exposed to control for 4 h. 5) The in-gel detection of NDPK. $n = 6 \pm$ SD, $p \leq 0.05$.

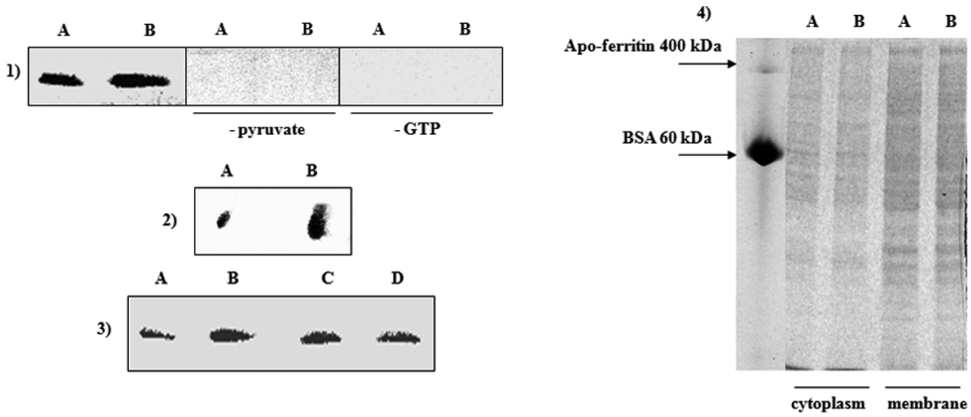

Figure 2. Activity and expression of PC in cells exposed to A) control or B) Al-stressed conditions. 1) In-gel activity stain analysis of PC. 2) 2D SDS PAGE analysis of PC protein levels. The bands from panel I were excised, treated with a 1% SDS solution, and then electrophoresed under denaturing conditions. Protein was detected using the silver staining protocol. 3) The Al-mediated modulation of PC activity: in-gel activity staining for cells exposed to A) control, B) Al-stressed, C) control exposed to Al-stressed, and D) Al-stressed exposed to control. 4) Coomassie stain of proteins to ensure equal loading and proper migration of cytoplasmic and membrane cell free extract.

termediates necessary for the biogenesis of the polycarboxylated aluminophore.

Similar to PC, ME and MDH displayed an increase in activity and expression in cells challenged with Al. Both of these enzymes play a crucial role in the metabolism of malate. While ME catalyzes the decarboxylation of malate to pyruvate in an NADP-dependent fashion, MDH produces NADH by the oxidation of malate to oxaloacetate. In the Al-treated cells, ME yielded a much sharper activity band in comparison to the control cells (Fig. 3, 1). The increase in activity correlated strongly with the increased expression of this enzyme. Indeed, 2D SDS PAGE analysis revealed a higher amount of protein associated with the activity bands from the Al-stressed cells (Fig. 3, 2). The in-gel activity analysis of MDH also produced a much more intense band in the Al-treated cells (Fig. 3, 3). Furthermore, the enhanced activity of this dehydrogenase was associated with an increase in protein expression (Fig. 3, 4).

The ability of *P. fluorescens* to tolerate Al toxicity is dependent on the production of an aluminophore which can render Al innocuous. However, Al is also known for its pro-oxidant activities. Thus, we hypothesized that exposure to Al would promote an increase in the activity of the NADP-producing enzyme, NADK. We have recently reported that NADK plays a crucial role in the generation of NADP following the exposure of

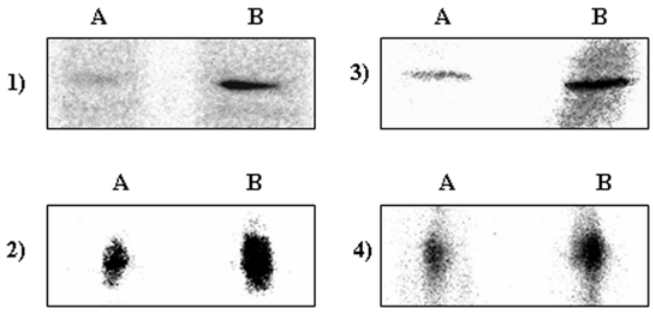

Figure 3. Activity and expression analysis of ME and MDH in cell exposed to A) control or B) Al-stressed conditions. 1) In-gel activity stain for ME. 2) 2D SDS PAGE analysis of ME protein levels. The bands from panel I were excised, treated with a 1% SDS solution, and then electrophoreses under denaturing conditions. Protein was detected using the silver staining protocol. 3) In-gel activity stain for MDH. 4) 2D SDS PAGE analysis of ME protein levels. The bands from panel III were excised, treated with a 1% SDS solution, and then electrophoreses under denaturing conditions. Protein was detected using the silver staining protocol.

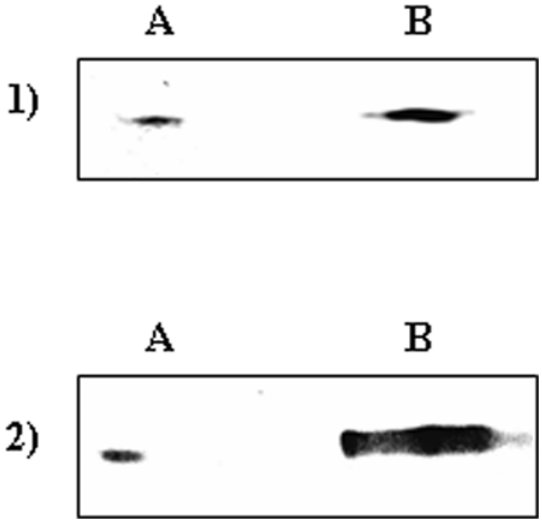

Figure 4. Activity analysis of enzymes involved in NADP homeostasis in cells exposed to A) control or B) Al-stressed conditions. 1) In-gel activity stain of NAD kinase. 2) In-gel activity stain for NADP-ICDH.

P. fluorescens to oxidative stress [18] In contrast to the control, the Al-exposed cells generated a much more intense activity band (Fig. 4, 1). Thus, Al toxicity promotes the conversion of NAD into NADP. Since ME, a known NADPH-generating enzyme, displayed an increase in activity, we also measured the activity of NADP-ICDH. We have recently shown that NADP-ICDH plays a crucial role in attenuating oxidative stress in cells exposed to ROS and metal toxicity [22]. Indeed, the activity of NADP-ICDH was increased in the cells exposed to Al (Fig. 4, 2). Thus, *P. fluorescens* exposed to Al evoke a metabolic shift aimed at quelling oxidative stress and detoxifying Al.

We have previously reported that several enzymes within the TCA cycle work in unison to convert citrate into an aluminophore [11]. Indeed, alterations in the activities of several TCA cycle and glyoxylate shunt pathway enzymes funnel acetyl-CoA and oxaloacetate towards the production of an Al-detoxifying agent. The regulation of TCA cycle enzymes by Fe and small RNA transcripts has also been shown [23]. Enzymes in this metabolic network have been demonstrated to confer resistance to vanadium in *P. fluorescens* [24]. However, the molecular mechanisms that lead to the homeostasis of oxaloacetate are not fully understood. This study shows that a sharp decrease in activity and expression of PEPCK and an upregulation in PC is an important component of this metabolic adaptation. The alteration of the activity and expression of these two enzymes would ensure that oxaloacetate is made readily available for the production of the aluminophore. Indeed, the lowering of PEPCK and increase in PC would dedicate this crucial metabolite to detoxifying Al instead of gluconeogenesis.

Furthermore, the lowering of NDPK activity would aid in preventing PEPCK activity by decreasing the levels of GTP or ATP. PC and PEPCK normally function in tandem in order to convert pyruvate into PEP for biosynthetic reactions leading to gluconeogenesis in an energy replete situation [25]. However, in this study, we show for the first time that *P. fluorescens* exposed to Al is capable of altering this critical metabolic module in order to detoxify this trivalent metal. Indeed, the ability of *P. fluorescens* to uncouple PC and PEPCK pro-

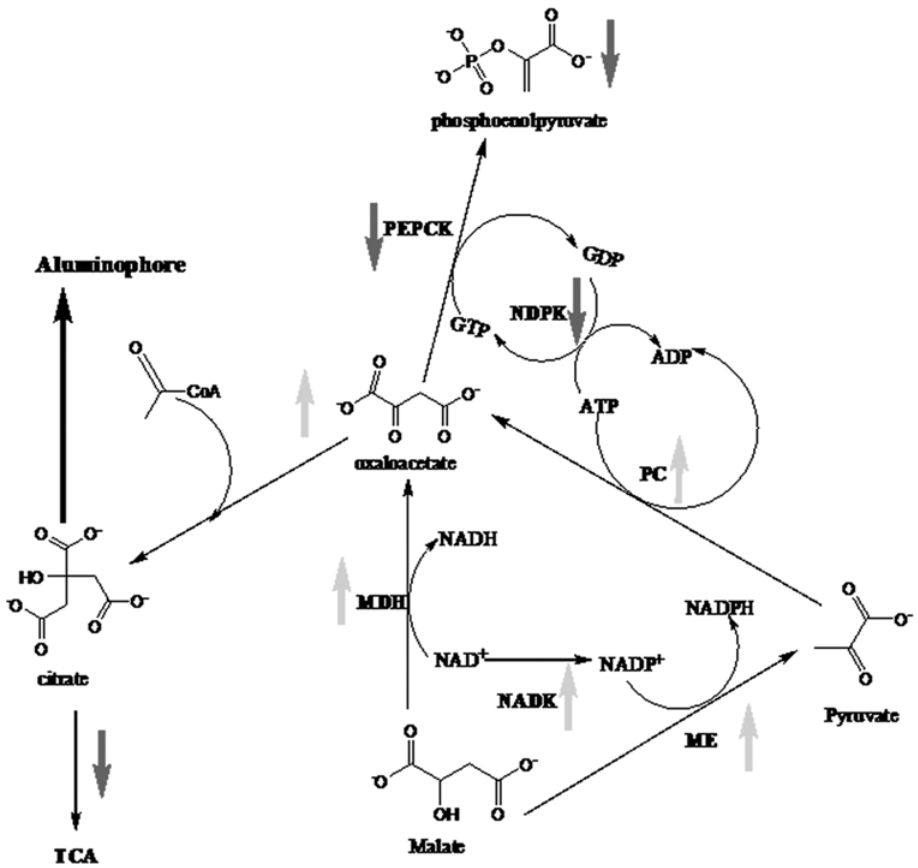

Figure 5. A metabolic adaptation favouring the production of oxaloacetate, a precursor for the genesis of the polycarboxylic aluminophore.

vides a novel insight into the adaptive response to a toxic environment. We have made similar observations with ICL and malate synthase (MS), two enzymes involved in the glyoxylate shunt [26]. In Al-stress, in order to produce oxalate to sequester Al, the activity of ICL is enhanced while that of MS is diminished [27]. This allows the glyoxylate to be utilized for the biogenesis of oxalate.

Since oxaloacetate is required for the production of the citrate derivative, we probed the activity and expression of the malate-metabolizing enzymes, MDH and ME. MDH displayed a sharp increase in activity and expression, which would aid in the contribution to the oxaloacetate pool. ME was also increased in activity and expression. An increase in ME would channel malate towards pyruvate, a scenario that would ensure the production of NADPH for ROS detoxification reactions [28]. Indeed, Al is known for its pro-oxidant activities and organisms exposed to this metal upregulate enzymes involved NADPH production [29]. Furthermore, pyruvate, a known antioxidant, can also be dedicated to ROS sequestration [30]. Thus, an increase in ME activity would provide this microbe with the necessary antioxidants to quell Al-induced oxidative stress. In addition, the pyruvate can be channelled back to oxaloacetate by PC. This would provide a metabolic response aimed at detoxifying ROS and maintaining oxaloacetate pools for the biogenesis of the aluminophore. The production of NADPH for ROS scavenging was aided by NADK and NADP-ICDH. NADK has been described as the sole producer of NADP in most organisms [31]. Furthermore, we have reported recently that this kinase plays a critical role in the response of both prokaryotes and eukaryotes to oxidative stress and metal toxicity [18, 20]. In the current study, NADK was upregulated in the Al-treated cells. This enzyme would supply the necessary NADP molecules for both ME and NADP-ICDH, thus participating in antioxidant defense.

In conclusion, this study demonstrates that Al-exposed *P. fluorescens* uncouples PC and PEPCK, a critical metabolic module involved in gluconeogenesis, in order to sustain oxaloacetate levels for aluminophore production. While PEPCK activity was decreased in order to maintain the oxaloacetate pool, PC was upregulated in order to convert pyruvate, a product of ME activity, into oxaloacetate. The metabolic adaptation of this soil microbe to an Al-containing medium is outlined in Fig. 5. Thus, a metabolic shift involving the uncoupling of PC and PEPCK and the upregulation of NADPH-generating enzymes enables *Pseudomonas fluorescens* to survive Al toxicity.

Acknowledgements

We gratefully acknowledge funding from The Ontario Centre of Excellence.

References

[1] Busselberg, D., 1995. Calcium channels as target sites of heavy metals. Toxicol. Lett., **82/83**, 255–261.

[2] Andrews, P.A., 2000. Disorders of iron metabolism. N. Engl. J. Med., **342**, 1293; author reply 1294.

[3] Yokel, R.A., 2000. The toxicology of aluminum in the brain: a review. Neurotoxicology, **21**, 813–828.

[4] Ward, R.J., Zhang, Y. and Crichton, R.R., 2001. Aluminium toxicity and iron homeostasis. J. Inorg. Biochem., **87**, 9–14.

[5] Anoop, V.M., Basu, U., McCammon, M.T., McAlister-Henn, L. et al., 2003. Modulation of citrate metabolism alters aluminum tolerance in yeast and transgenic canola overexpressing a mitochondrial citrate synthase. Plant Physiol., **132**, 2205–2217.

[6] de la Fuente, J.M., Ramirez-Rodriguez, V., Cabrera-Ponce, J.L. and Herrera-Estrella, L., 1997. Aluminum tolerance in transgenic plants by alteration of citrate synthesis. Science, **276**, 1566–1568.

[7] Kochian, L.V., Hoekenga, O.A. and Pineros, M.A., 2004. How do crop plants tolerate acid soils? Mechanisms of aluminum tolerance and phosphorous efficiency. Annu. Rev. Plant. Biol., **55**, 459–493.

[8] Hamel, R.D. and Appanna, V.D., 2001. Modulation of TCA cycle enzymes and aluminum stress in Pseudomonas fluorescens. J. Inorg. Biochem., **87**, 1–8.

[9] Appanna, V.D. and Pierre, M.S., 1996. Aluminum elicits exocellular phosphatidylethanolamine production in *Pseudomonas fluorescens*. Appl. Environ. Microbiol., **62**, 2778–2782.

[10] Appanna, V.D. and Pierre, M.S., 1994. Influence of phosphate on aluminum detoxifiction of *Pseudomonas fluorescens*. FEMS Microbiology Letters, **124**, 327–332.

[11] Appanna, V.D., Hamel, R., Mackenzie, C., Kumar, P. *et al.*, 2003. Adaptation of *Pseudomonas fluorescens* to Al-citrate: involvement of tricarboxylic acid and glyoxylate cycle enzymes and the influence of phosphate. Curr. Microbiol., **47**, 521–527.

[12] Anderson, S., Appanna, V.D., Huang, J. and Viswanatha, T., 1992. A novel role for calcite in calcium homeostasis. FEBS Lett., **308**, 94–96.

[13] Sapan, C.V., Lundblad, R.L. and Price, N.C., 1999. Colorimetric protein assay techniques. Biotechnol. Appl. Biochem., **29** (Pt 2), 99–108.

[14] Romanov, V., Merski, M.T. and Hausinger, R.P., 1999. Assays for allantoinase. Anal. Biochem., **268**, 49–53.

[15] Schagger, H. and von Jagow, G., 1991. Blue native electrophoresis for isolation of membrane protein complexes in enzymatically active form. Anal. Biochem., **199**, 223–231.

[16] Singh, R., Chenier, D., Beriault, R., Mailloux, R. *et al.*, 2005. Blue native polyacrylamide gel electrophoresis and the monitoring of malate- and oxaloacetate-producing enzymes. J. Biochem. Biophys. Methods, **64**, 189–199.

[17] Mailloux, R., Lemire, J. and Appanna, V., 2007. Aluminum-induced mitochondrial dysfunction leads to lipid accumulation in human hepatocytes: a link to obesity. Cell. Physiol. Biochem., **20**, 627–638.

[18] Singh, R., Mailloux, R.J., Puiseux-Dao, S. and Appanna, V. D., 2007. Oxidative stress evokes a metabolic adaptation that favors increased NADPH synthesis and decreased NADH production in *Pseudomonas fluorescens*. J. Bacteriol., **189**, 6665–6675.

[19] Laemmli, U.K., 1970. Cleavage of structural proteins during the assembly of the head of bacteriophage T4. Nature, **227**, 680–685.

[20] Mailloux, R. J., Singh, R. and Appanna, V.D., 2006. In-gel activity staining of oxidized nicotinamide adenine dinucleotide kinase by blue native polyacrylamide gel electrophoresis. Anal. Biochem., **359**, 210–215.

[21] Dzeja, P.P. and Terzic, A., 2003. Phosphotransfer networks and cellular energetics. J. Exp. Biol., **206**, 2039–2047.

[22] Mailloux, R.J., Beriault, R., Lemire, J. and Singh, R. *et al.*, 2007. The tricarboxylic acid cycle, an ancient metabolic network with a novel twist. PLoS ONE, 2, e690.

[23] Vasil, M.L., 2007. How we learnt about iron acquisition in *Pseudomonas aeruginosa*: a series of very fortunate events. Biometals, **20**, 587–601.

[24] Denayer, S., Matthijs, S. and Cornelis, P., 2006. Resistance to vanadium in *Pseudomonas fluorescens* ATCC 17400 caused by mutations in TCA cycle enzymes. FEMS Microbiol. Lett., **264**, 59–64.

[25] Owen, O.E., Kalhan, S.C. and Hanson, R.W., 2002. The key role of anaplerosis and cataplerosis for citric acid cycle function. J. Biol. Chem., **277**, 30409–30412.

[26] Hamel, R., Appanna, V.D., Viswanatha, T. and Puiseux-Dao, S., 2004. Overexpression of isocitrate lyase is an important strategy in the survival of *Pseudomonas fluorescens* exposed to aluminum. Biochem. Biophys. Res. Commun., **317**, 1189–1194.

[27] Hamel, R., Levasseur, R. and Appanna, V.D., 1999. Oxalic acid production and aluminum tolerance in *Pseudomonas fluorescens*. J. Inorg. Biochem., **76**, 99–104.

[28] Sies, H., 1993. Strategies of antioxidant defense. Eur. J. Biochem., **215**, 213–219.

[29] Singh, R., Beriault, R., Middaugh, J., Hamel, R. *et al.*, 2005. Aluminum-tolerant *Pseudomonas fluorescens*: ROS toxicity and enhanced NADPH production. Extremophiles, **9**, 367–373.

[30] Tejero-Taldo, M.I., Caffrey, J.L., Sun, J. and Mallet, R.T., 1999. Antioxidant properties of pyruvate mediate its potentiation of beta-adrenergic inotropism in stunned myocardium. J. Mol. Cell Cardiol., **31**, 1863–1872.

[31] Pollak, N., Dolle, C. and Ziegler, M., 2007. The power to reduce: pyridine nucleotides-small molecules with a multitude of functions. Biochem. J., **402**, 205–218.

